PIBB 生物化学与生物物理进展
Progress in Biochemistry and Biophysics
2019,46(6):612~619
www.pibb.ac.cn

High-Dynamic Optical Angiography*

ZENG Ya-Guang**, LUO Jia-Xiong, HAN Ding-An, XIONG Hong-Lian, WANG Xue-Hua, ZHONG Jun-Ping, WANG Ming-Yi**

(*School of Physics and Optoelectronic Engineering, Foshan University, Foshan* 528000, China)

Abstract We propose a high-dynamic optical angiography(HDOA) method to obtain blood flow images of a small biological specimen *in vivo*. High dynamic range exposure time is set to achieve high-dynamic integrated time modulation, which involves dynamic integrated effect and absorption effect. With this method, each-level vessels can be imaged with similar clarity. Moreover, the vessels in locations with different thickness and absorption coefficient can be reconstructed in the same image. Experiments on phantom and *in vivo Gold Pristella Tetra* were performed to demonstrate that HDOA can achieve each-level vessels imaging based on dynamic integrated effect and absorption effect.

Key words high-dynamic optical angiography, high-dynamic integrated time modulation, absorption effect
DOI: 10.16476/j.pibb.2019.0074

Hemodynamic research is of great importance in basic studies in the field of life sciences[1-2]. Microcirculation studies have shown that hemodynamic changes can reflect the state of function of the organism[3-6]. For example, diseases such as diabetes and high blood pressure can cause changes in the vascular structure before complications occur in the heart and kidneys[7-10]. The field of vascular structure research will directly benefit from high-resolution microangiography imaging. The laser speckle contrast imaging(LSCI) method enables full-field two-dimensional high-temporal resolution blood flow imaging without scanning or in a non-contact mode[11]. This technique has found important applications in the functional research of biological tissues such as the cortex and fundus retina, and is an important tool for basic research in life sciences[12-15]. Because LSCI uses wide field illumination instead of point illumination, it is suitable for flow imaging of shallow layers in relatively transparent media. Rice *et al.* [16] proposed a combination of multiple exposure speckle imaging and spatial frequency analysis to resolve moving particles at a certain depth and improve the depth of blood flow imaging. In addition, in order to improve the ability of laser speckle contrast imaging to quantify blood flow rate, Parthasarathy *et al.* [17] utilized a multi-exposure speckle imaging method. This method uses the original speckle image obtained under different exposure time conditions to calculate the contrast ratio, and then fits the contrast ratio with the exposure time to approximate the autocorrelation function of the light field. The method can overcome the shortcoming of small dynamic range in single exposure imaging, and can be used to obtain more accurate two-dimensional blood flow distribution images with different flow rates. However, these multi-exposure speckle imaging methods use long exposure times for acquisition, so that the blood flow signal is blurred, and cannot achieve high-resolution angiography[18-19]. Recently, a method of intensity fluctuation modulation laser speckle imaging(LSI-IFM) based on short exposure has been proposed and its ability for optical microangiography imaging has been demonstrated[20-21]. Short exposures ensure that transient dynamic speckle signals are captured.

* This work is supported by grants from The National Natural Science Foundation of China (61605026, 11474053, 61471123, 61771139, 81601534, 61705036), Natural Science Foundation of Guangdong Province (2015A030313639, 2017A030313386) and the College Students Innovation and Entrensurship Training Program of Guangdong Province (XJ2018039).
** Corresponding author. Tel: 86-757-82716895
ZENG Ya-Guang. E-mail: zeng.yg @163.com
WANG Ming-Yi. E-mail: wangmingyi@mail.bnu.edu.cn
Received: April 9, 2019 Accepted: May 5, 2019

However, short exposure times do not allow penetrating imaging samples with a certain thickness, and only shallow layers of relatively transparent samples can be imaged; the technique is also susceptible to dynamic signal changes.

In this Letter, we report a high-dynamic optical angiography(HDOA) method based on high-dynamic integrated time modulation to image micro-vessel networks. This method can be applied for specimens with non-uniform thickness and absorption coefficient. In addition, high-dynamic integrated time can eliminate the effect of large velocity differences between different-level vessels, so that big vessels and capillaries can be resolved simultaneously with similar SNR. In practical applications, HDOA is beneficial for biomedical research on laboratory animals, for example, study of angiogenesis in fish.

1 Materials and methods

A schematic diagram of the experimental setup is shown in Figure 1a. A semiconductor laser (λ = 690 nm, 100 mW, Changchun New Industries Optoelectronics Technology, China), is expanded by a beam expander (BE), and then illuminates the specimen. The diffuse reflective light is relayed by a microscope (Olympus SZ-CTV) onto an 8-bit CMOS camera (acA2000-340 km, Basler). The camera has a frame size of 2 048 × 1 088 pixels, with a 5.5 μm × 5.5 μm pixel size and a 42 fps(frames/second) frame rate. The microscope lens magnification can be adjusted within the range 0.75−2.5. The entire experimental setup is fixed on a vibration-free optical platform to reduce the effects of external vibration on the imaging.

The acquired signal can be considered as fragments of a Doppler signal, so that it is a superposition of signals with different frequencies. The dynamic integrated time influence the intensity and frequency distribution of the acquired signal. Therefore, a series of exposure time gradients were set in this method. As shown in Figure 1b, under each exposure time, raw speckle images of 512 frames were acquired and processed to obtain a blood flow image. In total, 512N frames images were continuously acquired to reconstruct N blood flow images. For the nth exposure time, the raw signal of one camera pixel can be expressed as $I_n(t)$:

$$I_n(t) = \left[I_0 + \sum_{i=1}^{m} I_i \cos\left(2\pi f_i t\right) \prod_{\frac{T_n}{2}} \left[t - t_0 \right] \right] \quad (1)$$

where I_0 is the background signal, which is the so-called stationary signal, and $\sum_{i=1}^{n} I_i \cos\left(2\pi f_i t\right) \prod_{\frac{T_n}{2}} \left[t - t_0 \right]$ is the dynamic signal generated by moving scattering particles. $\prod_{\frac{T_n}{2}} \left[t - t_0 \right]$ is a block-pulse function defined a $rect\left[2\left(t - t_0\right)/T_n \right] * comb\left(vt\right)$, where t_0 is the initial time point, n is the gradient number of exposure time, T_n is the nth exposure time, v is the sampling rate of our camera, and "*" denotes convolution. The captured signal can be considered to be generated as a result of the camera integrating the number of received photons. As the exposure time increases,

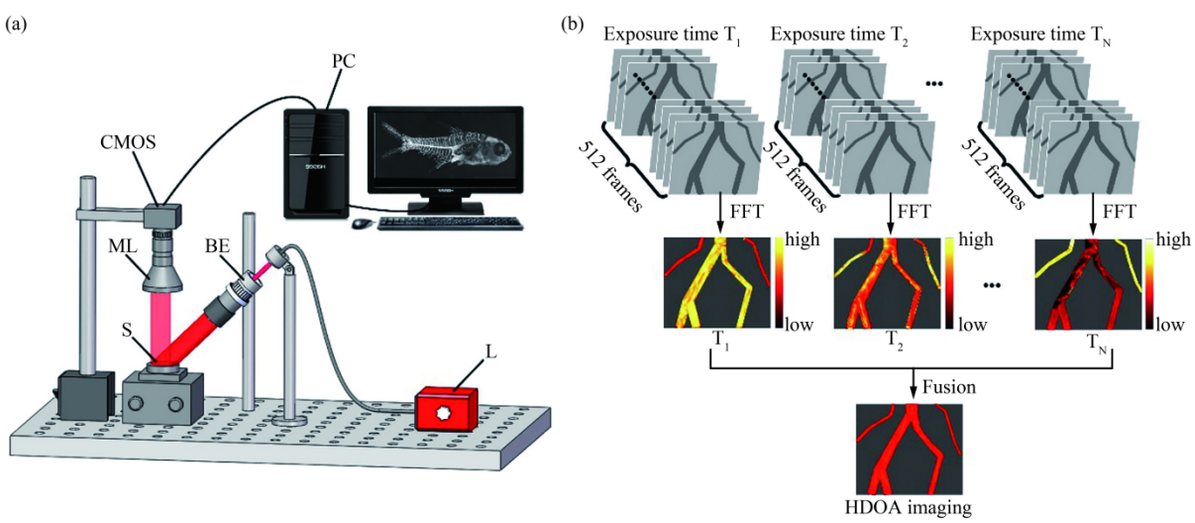

Fig. 1 Schematic of the HDOA method

(a) Schematic of the experimental setup. (b) The operating principle of the HDOA method.

I_0 and the mean value of $I_n(t)$ increase. In order to analyze the effect of dynamic integrated time on the stationary and dynamic signals, fast Fourier transform was performed to convert the raw speckle pattern recorded at each pixel from the time domain to the frequency domain:

$$FFT_{t\to u}[\,I_n(t)\,] = i_s[u] + i_d\left[u \pm f_i\right] \quad (2)$$

Where $i_s[u]$ is a frequency-domain stationary signal and $i_d\left[u \pm f_i\right]$ is a frequency-domain dynamic signal. In the frequency domain, $i_s[u]$ increases as the exposure time increases. This results from the increasing stationary signal contribution. Besides, dynamic signal also plays an important role. Longer exposure time blurs the dynamic signal, especially for the one corresponding to high-velocity flow, and transforms it to low-frequency signal. For each exposure time, the imaging parameter, MD_n, is defined as the ratio of the average intensity of the frequency-domain dynamic signal to that of the stationary signal.

$$MD_n = \frac{\left\langle i_d\left[u \pm f_i\right]\right\rangle_{f_0\sim f/2}}{\left\langle i_s[u]\right\rangle_{0\sim f_0}} \quad (3)$$

Where f_0 and f are the filter range and camera sampling rate, respectively. MD_n of each-level vessels vary as the exposure time increases from T_1 to T_n. As shown in Figure 1b, MD_n of small vessels increases and that of big vessels decreases as the exposure time increases. In the common biomedical condition, the interference signal frequency is typically in the range of 20 Hz−10 kHz[22]. For a short exposure time, MD_n remains almost same with increasing flow velocity. Because the exposure time (*e.g.*, 0.1 ms) is short enough to capture the instantaneous high-frequency Doppler signal. However, for a long exposure time, MD_n decreases rapidly as the flow velocity increases. For example, an exposure time of 5 ms is used in laser speckle contrast analysis imaging. Considering both the dynamic integrated effect and absorption effect, a short exposure time is more suitable for big vessels with high velocity and a long exposure time is more appropriate for small vessels with low red blood cells concentration and absorption coefficient. To integrate the superior high-dynamic information, a series of images with multi-exposure time were fused into a HDOA image. The imaging parameter, high-dynamic modulation depth (HDMD), is defined as:

$$\mathrm{HDMD}(x,y) = \max\left[MD_n(x,y)\right]_{blood} + \min\left[MD_n(x,y)\right]_{background} \quad (4)$$

First, the configuration of blood flows are extracted from the background. Second, the highest $MD_n(x,y)$ of the same blood flows and the lowest pixel value $MD_n(x,y)$ of the same background location in multi-exposure images are selected to reconstruct the HDOA image.

2 Experiment and results

The dependence between the dynamic integrated time and the imaging quality of each-level vessels was verified by a phantom experiment with designed flow velocity and scattering particles concentration. Two capillary tubes with the inner diameter of 0.5 mm were fixed in 2% agarose gel for index matching. As shown in Figure 2a, 0.8 g/L and 1.6 g/L TiO_2 solutions were injected into tube A and tube B, by a double-channel syringe pump (JZB-2800, JYM), with the velocity of 2.8 mm/s and 8.4 mm/s, respectively. Tube A was used to simulate a capillary with a low RBC concentration and flow velocity, and tube B corresponds to a big vessel with a high RBC concentration and flow velocity. Figure 2b shows the relationship between the MD and the exposure time for tube A and tube B. The exposure time increases from 120 μs to 700 μs with same gradient of 58 μs. The MD results from the average value of the area indicated by the dashed-line box in Figure 2a. For tube A, MD is directly proportional to the exposure time, and for tube B, the relationship is inverse. Two factors should be considered for this result. The first is the absorption effect and the second is the dynamic integrated effect. For tube A, the flow velocity is sufficiently low that a long exposure time almost does not blur the dynamic signal. Meanwhile, long exposure time increases the dynamic signal amplitude, which is too weak to be acquired for a low exposure time. Similarly, for tube B, MD considerably decreases owing to the high dynamic integrated effect shown for a high flow velocity. Correspondingly, for different level vessels, a big vessel has high RBCs concentration and flow velocity, and microvessel has low RBCs concentration and flow velocity. Therefore, we assume that the MD of vessels decreases as the exposure time increases, and the MD of microvessels increases as the exposure time increases.

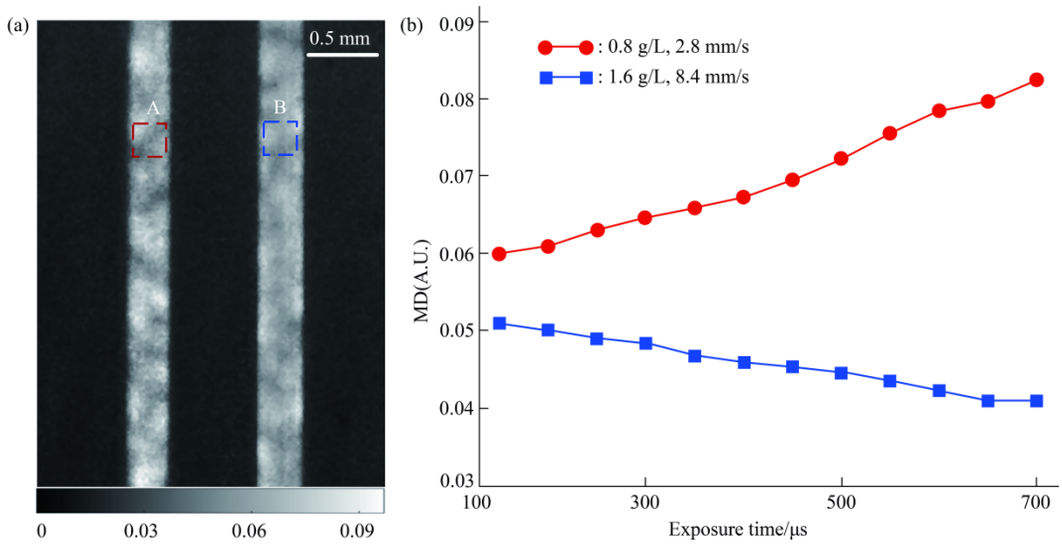

Fig. 2 Phatom experiment images

(a) MD image of the phantom. (b) Relationship between the average MD and the exposure time at different concentrations and flow speed.

To demonstrate the influence of absorption on imaging, we imaged the blood flow of a twenty-day-old *Gold Pristella Tetra*. The *Gold Pristella Tetra* was anesthetized with 5 mg/L stabilizer (MS-222). Then, it was fixed in a plastic dish filled with low melting-point agarose L.M.P (1% agar gel, temperature 24℃) to minimize the impact of its movement on the imaging. Figure 3a is a raw acquired image of the fish. Figure 3b-e shows the MD image obtained at the exposure time of 0.05, 0.25, 0.35 and 0.50 ms, respectively. Figure 3f shows the HDMD image using the HDOA imaging method. According to Lambert-Beer's law, samples of different thicknesses and absorption coefficients have different transmittances of light. We selected three regions of the *Gold Pristella Tetra* (P1, P2, and P3) to compare the imaging differences between the MD and the HDMD images. P1, P2, and P3 are related to fish mouse, swim bladder, and fish tail, respectively. P1 and P2 have similar thickness; however, the difference between their absorption coefficients is significant. The difference between the thicknesses of P2 and P3, is very high. For any single exposure time, these vessels in P1, P2, and P3 cannot be imaged simultaneously. However, HDOA can extract the optimal information at different absorption conditions and reconstruct all vessels in a HDMD image. To illustrate the effect of absorption on HDOA, we quantitively analyze the spatial resolution and signal noise ratio of P1, P2, and P3. Figure 3g−h shows the spatial resolution and signal-to-noise ratio (SNR) of the MD image at the exposure time of 0.05, 0.25, 0.35 and 0.50 ms and the HDMD image, respectively. The pixel values of the regions indicated by the dashed-line boxes in Figure 3b−e are used to calculate the spatial resolution and SNR. The calculation method of spatial resolution is described as follows. We select the data of a region to obtain the MD curve, where the difference between the half-height and the quarter-height of the obtained curve peak is defined as the spatial resolution. Note that in Figure 3h the HDMD image has a higher SNR and its SNR increases with the exposure time. This verifies the feasibility of the HDOA method for obtaining high-resolution blood flow imaging.

To demonstrate the influence of high dynamic effect on imaging, we present an enlarged view of the *Gold Pristella Tetra* and analyze different-level vessels. The magnification of the microscope is set to 1.8. Figure 4a shows the HDMD image of the *Gold Pristella Tetra*. In this figure, M represents the area of the microvessel, and V represents the area of the

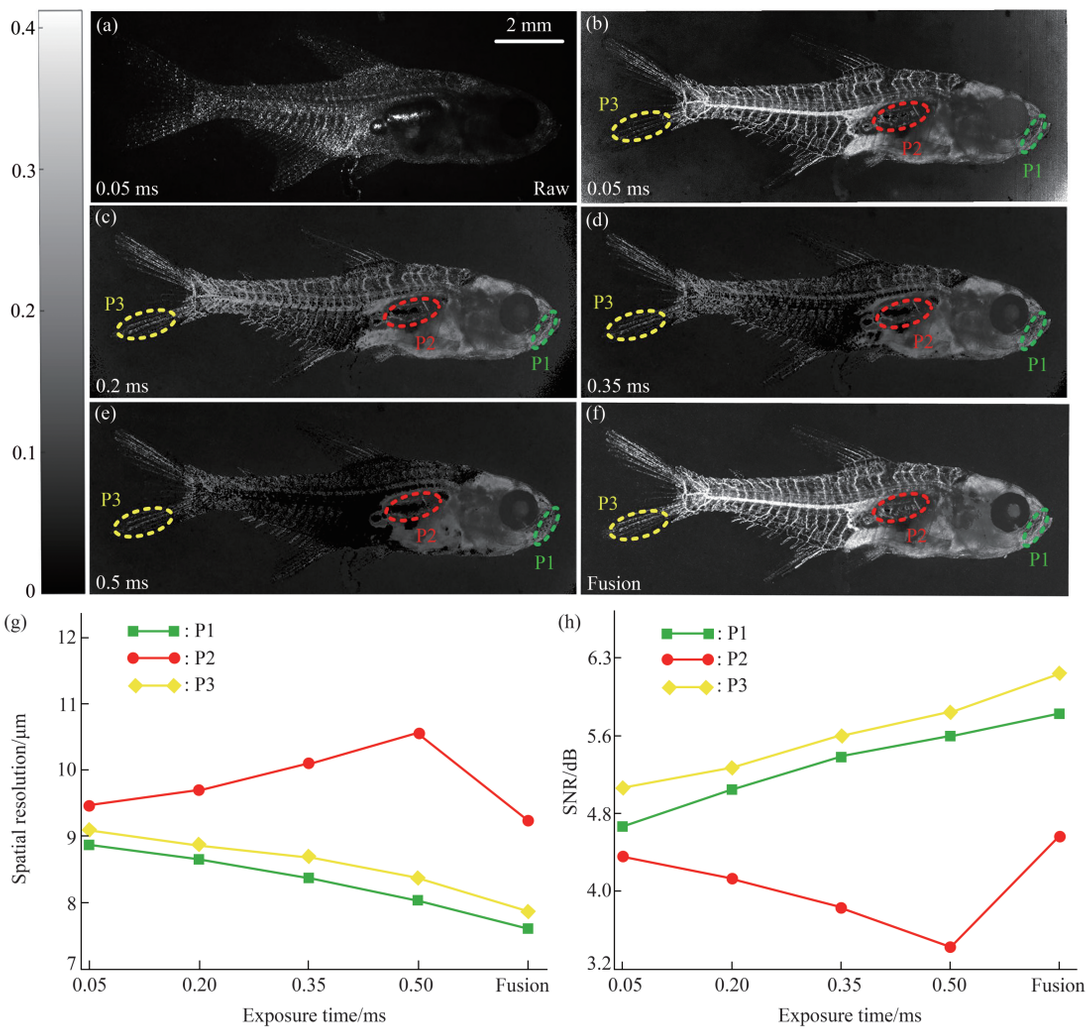

Fig. 3　High-dynamic angiography with HDOA imaging method

（a）Raw acquired image.（b-e）MD image obtained at exposure times of 0.05, 0.25, 0.35 and 0.50 ms, respectively.（f）HDMD image.（g-h）Spatial resolution and SNR corresponding to the three regions shown in the dashed-line boxes in（b-e）.

vessel. To facilitate the observation of the blood vessel distribution of the *Gold Pristella Tetra* at different exposure times, we present a view of the area indicated by the solid-line box(Figure 4a) at different exposure times. Figure 4b-g show the MD images obtained at exposure times of 0.024, 0.2, 0.4, 0.6, 0.8, and 1.0 ms. Arrow A and arrow B represent the area of the vessel and microvessel, respectively. As the exposure time increases, over-exposure occurs in vessel, and the clarity of microvessel improves gradually. The acquired signal of RBCs flowing with high velocities in large vessels fluctuates with high frequency. When a short exposure time is used in the experiment, the fluctuated fragments of the Doppler signal can be acquired. However, the acquired Doppler signal must be blurred as exposure time increases. In this case, the imaging parameter MD will decrease, as the integration of more signals eliminates the fluctuation of the acquired signal. For RBCs with low flow velocities, an increase in the exposure time does not lead to the blurring of the acquired signal. Instead, it enlarges the acquired signal and improve its sensitivity. Figure 4h shows the exposure time required for the imaging of vessel and microvessel in the dashed-line box in Figure 4a. From it we can found that the data of microvessels is mainly acquired

under long exposure time, while the one of vessel mainly from shorter exposure time. The conclusion also coincides with the assumption made in the phantom experiment.

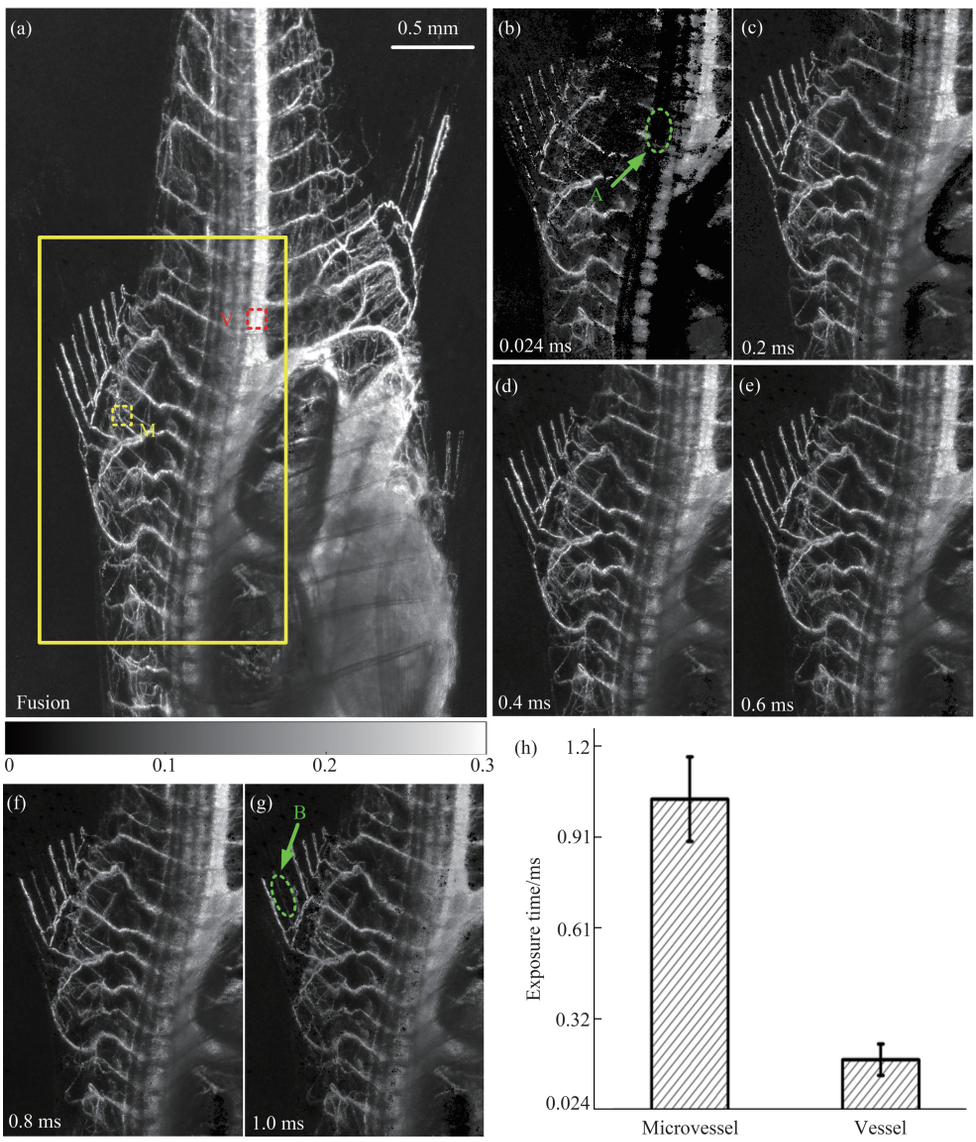

Fig. 4 Local high−dynamic angiography

(a) HDMD image of *Gold Pristella Tetra*. (b-g) MD image of the region in the solid-line rectangle in (a) at exposure times of 0.024, 0.2, 0.4, 0.6, 0.8 and 1.0 ms, respectively. (h) The optimal exposure time required for imaging of vessel and microvessel in the dashed-line rectangle in (a). Arrow A and arrow B represent the area of the vessel and microvessel, respectively.

3 Discussion and conclusion

In conclusion, we have proposed a HDOA method, which can perform blood flow imaging for specimens with different thicknesses and absorption coefficients. The high performance of the proposed method was verified by a phantom and an *in vivo* biological experiments. However, the proposed HDOA method also has its limitations. For example, the biological tissue must be thin or neartransparent, and its imaging time is affected by the multiple exposure time acquisition mechanism.

References

[1] Magder S. Hemodynamic monitoring in the mechanically ventilated patient. Current Opinion in Critical Care, 2011, **17**(1): 36-42

[2] Martin C, Martindale J, Berwick J, *et al*. Investigating neural-hemodynamic coupling and the hemodynamic response function in the awake rat. Neuroimage, 2006, **32**(1): 33-48

[3] Qin J, Reif R, Zhi Z, *et al*. Hemodynamic and morphological vasculature response to a burn monitored using a combined dual-wavelength laser speckle and optical microangiography imaging system. Biomedical Optics Express, 2012, **3**(3): 455-466

[4] Segal S S. Regulation of blood flow in the microcirculation. Microcirculation, 2005, **12**(1): 33-45

[5] Secomb, Timothy W. Blood flow in the microcirculation. Annual Review of Fluid Mechanics, 2017, **49**(1): 443-461

[6] Liu R, Huang Q, Li B, *et al*. Extendable, miniaturized multi-modal optical imaging system: cortical hemodynamic observation in freely moving animals. Optics Express, 2013, **21**(2): 1911-1924

[7] Gómez-Marcos Manuel, Recio-Rodríguez José, Patino-Alonso María, *et al*. Cardio-ankle vascular index is associated with cardiovascular target organ damage and vascular structure and function in patients with diabetes or metabolic syndrome, LOD-DIABETES study: a case series report. Cardiovascular Diabetology, 2015, **14**(1): 1-10

[8] El-Asrar M A, Ismail E A R, Thabet R A, *et al*. Osteopontin as a marker of vasculopathy in pediatric patients with type 1 diabetes mellitus: relation to vascular structure. Pediatric Diabetes, 2018, **19**(6): 1107-1115

[9] Noon J P, Walker B R, Webb D J, *et al*. Impaired microvascular dilatation and capillary rarefaction in young adults with a predisposition to high blood pressure. Journal of Clinical Investigation, 1997, **99**(8): 1873-1879

[10] Urbina, Elaine M. Abnormalities of vascular structure and function in pediatric hypertension. Pediatric Nephrology, 2016, **31**(7): 1061-1070

[11] Briers, J. D. Laser speckle contrast analysis (LASCA): a nonscanning, full-field technique for monitoring capillary blood flow. Journal of Biomedical Optics, 1996, **1**(2): 174-179

[12] Dunn A K, Bolay H, Moskowitz M A, *et al*. Dynamic imaging of cerebral blood flow using laser speckle. Journal of Cerebral Blood Flow & Metabolism, 2001, **21**(3): 195-201

[13] Li P, Ni S, Zhang L, *et al*. Imaging cerebral blood flow through the intact rat skull with temporal laser speckle imaging. Optics Letters, 2006, **31**(12): 1824-1826

[14] Ponticorvo A, Cardenas D, Dunn A K, *et al*. Laser speckle contrast imaging of blood flow in rat retinas using an endoscope. Journal of Biomedical Optics, 2013, **18**(9): 090501

[15] Neganova A Y, Postnov D D, Olga S, *et al*. Rat retinal vasomotion assessed by laser speckle imaging. Plos One, 2017, **12**(3): e0173805

[16] Rice T B, Kwan E, Hayakawa C K, *et al*. Quantitative, depth-resolved determination of particle motion using multi-exposure, spatial frequency domain laser speckle imaging. Biomedical Optics Express, 2013, **4**(12): 2880-2892

[17] Parthasarathy A B, Tom W J, Gopal A, *et al*. Robust flow measurement with multi-exposure speckle imaging. Optics Express, 2008, **16**(3): 1975-1989

[18] Yuan S, Devor A, Boas D A, *et al*. Determination of optimal exposure time for imaging of blood flow changes with laser speckle contrast imaging. Applied Optics, 2005, **44**(10): 1823-1830

[19] Kazmi S M S, Balial S, Dunn A K. Optimization of camera exposure durations for multi-exposure speckle imaging of the microcirculation. Biomedical Optics Express, 2014, **5**(7): 2157-2171

[20] Zeng Y , Wang M , Feng G , *et al*. Laser speckle imaging based on intensity fluctuation modulation. Optics Letters, 2013, **38**(8): 1313-1315

[21] Wang M, Zeng Y, Liang X, *et al*. *In vivo* label-free microangiography by laser speckle imaging with intensity fluctuation modulation. Journal of Biomedical Optics, 2013, **18**(12): 126001

[22] Serov A, Steinacher B, Lasser T. Full-field laser Doppler perfusion imaging and monitoring with an intelligent CMOS camera. Optics Express, 2005, **13**(10): 3681-3689

高动态光学血管造影成像*

曾亚光**　罗佳雄　韩定安　熊红莲　王雪花　钟俊平　王茗祎**

（佛山科学技术学院物理与光电工程学院，佛山 528000）

摘要　我们提出一种高动态光学血管造影成像（HDOA）方法来实现活体生物样本血管造影成像.该方法通过设置高动态范围曝光时间，依据动态积分效应和吸收效应以实现高动态积分时间调制.通过该方法，不仅能够同时获得各级血管清晰的造影图像，还能消除样品厚度不均、吸收系数不同对成像造成的影响.论文以仿体和活体金鱼为样品，通过实验验证了HDOA方法根据动态积分调制效应和吸收效应，能有效实现各级血管同时成像.

关键词　高动态光学血管造影成像，高动态积分时间调制，吸收效应

中图分类号　Q334　　**DOI**：10.16476/j.pibb.2019.0074

*国家自然科学基金（61605026，11474053，61471123，61771139，81601534，61705036），广东省自然科学基金（2015A030313639，2017A030313386）和广东省大学学生创新创业训练项目（XJ2018039）资助.

**通讯联系人. Tel：0757-82716895

曾亚光. E-mail：zeng.yg @163.com

王茗祎. E-mail：wangmingyi@mail.bnu.edu.cn

收稿日期：2019-04-09，接受日期：2019-05-05